ISSN 1996-3416

International Journal of Chemical Technology

http://knowledgiascientific.com

Knowledgia SCIENTIFIC
A Place to Publish Outstanding Research

OPEN ACCESS International Journal of Chemical Technology

ISSN 1996-3416
DOI: 10.3923/ijct.2018.1.22

Research Article
Adsorption of Chromium Using Blue Green Algae-Modeling and Application of Various Isotherms

[1]Ramsenthil Ramadoss and [2]Dhanasekaran Subramaniam

[1]Department of Chemical Engineering, Faculty of Engineering and Technology, Bioprocess Laboratory, Annamalai University, 608002 Annamalai Nagar, Tamil Nadu, India
[2]Department of Chemical Engineering, Faculty of Engineering and Technology, Mass Transfer Laboratory, Annamalai University, 608002 Annamalai Nagar, Tamil Nadu, India

Abstract

Background and Objectives: Cr (VI) is identified as one of the toxic heavy metal that is discharged into the environment. Adsorption technique is one of the ideal methods for removal of heavy metals because of its efficiency and low cost. A variety of materials have been tried as adsorbents for removal of Cr (VI). Blue Green Marine Algae (BGMA) is chosen as adsorbent and aimed to investigate its maximum adsorption capacity for adsorption of Cr (VI) from its synthetic stock solutions. **Materials and Methods:** The metal adsorption capacities of BGMA for adsorption of Cr (VI) ion were studied by varying the initial metal ion concentration from 25-250 ppm. All the experiments were performed at room temperature. To forecast the adsorption isotherms for modeling and to establish the characteristic parameters for process design various models were studied. **Results:** The optimum pH, biomass loading and an agitation rate for maximum removal of Cr (VI) ion were found to be 5, 2 g and 120 rpm, respectively. Freundlich isotherm was more apt than all other models investigated in this study. **Conclusion:** L shape of the isotherm indicated that there was no strong competition between solvent and Cr (VI) to occupy the active site s of BGMA. Also it was concluded that BGMA had a limited sorption capacity for adsorption of Cr (VI). Concurrence of Freundlich isotherm with experimental data indicated the extent of heterogeneity of the BGMA surface. The n_F value indicated that the adsorption of Cr (VI) from its synthetic solution onto BGMA was favourable one.

Key words: Water pollution, adsorption, isotherm models, chromium, blue green marine algae, heavy metal contamination

Citation: Ramsenthil Ramadoss and Dhanasekaran Subramaniam, 2018. Adsorption of chromium using blue green algae-modeling and application of various isotherms. Int. J. Chem. Technol., 10: 1-22.

Corresponding Author: Dhanasekaran Subramaniam, Department of Chemical Engineering, Faculty of Engineering and Technology, Mass Transfer Laboratory, Annamalai University, 608002 Annamalai Nagar, Tamil Nadu, India Tel: +91 99 426 26 198

Competing Interest: The authors have declared that no competing interest exists.

Data Availability: All relevant data are within the paper and its supporting information files.

INTRODUCTION

Water pollution by heavy metal contamination is a serious threat to mankind and aquatic life. The present study is aimed to focus the contamination by chromium. Tanning and leather industries, electroplating industries, catalyst and pigments manufacturing industries, fungicides, ceramics, crafts, glass, photography and corrosion control application are main sources for Chromium[1-3]. These industrial effluents can contain Cr (VI) from 10-100 mg L^{-1} which is higher than the standard limit of 0.1 mg L^{-1} in industrial waste water[4-6]. Chromium is a transition metal. It transpires in nine different forms of its oxidation states. The range is found to be Cr (-II) up to Cr (+VI). The Cr (III) and Cr (VI) oxidation states are the most commonly observed in chromium compounds. In aqueous systems contamination with chromium is mainly found as Cr (III) and Cr (VI). The remaining forms are rare states[1]. Cr (III) is considered as a bioelement since it plays an important role in the metabolic activity of plants and animals at its low concentrations[7-9]. But Cr (VI) is highly toxic[10-13].

According to report submitted by IARC[14-16], Cr (VI) is classified in Group 1 (carcinogenic to humans) and chromium (III) is classified in Group 3 (not carcinogenic to humans). The maximum permissible limit of Cr (VI) for discharge to land surface water is 0.1 mg L^{-1} and in potable water 0.05 mg L^{-1} [17-20]. Hence utmost attention is emerged in the removal of chromium (VI) from wastewater before discharge into the aquatic system. Ion exchange, membrane separation, dialysis and electro dialysis reduction followed by chemical precipitation, electro coagulation and adsorption/filtration are the conventional treatment technologies to remove Cr (VI) from water and wastewater[21-24]. Among the various conventional methods, adsorption is documented as the most efficient, promising and widely used fundamental technique. It is simple and cost effective for recovering and eliminating heavy metal ions from dilute solutions[25-28]. Understanding the basic mechanism of adsorption is also simple. It is a surface phenomenon in which one or more components present in a multi-component fluid (gas or liquid) mixture is attracted to the surface of solid adsorbents via physical or chemical bonds[29-32]. The presence of metal ions in aqueous media and subsequent development of pollution measures have resulted in the success of adsorption process. Studies with various bio sorbents are abundant in literature which includes seaweeds, moulds, yeast, bacteria, crab shells and agricultural products so on[33-35].

Marine macro-algae are harvested or cultivated in many parts of the world and are therefore readily available in large quantities for the development of highly effective bio sorbent materials[13]. The microalgae which exist in the freshwater environment and in the oceans are important in global ecology, extremely efficient and taxonomically diverse[36-39].

The investigation of adsorption capacities of various adsorbents for the removal chromium has been made conventionally with study of two parameter models. Extensive investigation have been made by various researchers in evaluating the characteristics of specific adsorbent-adsorbate systems and evaluating the degree of applicability of two parameter models for the systems concerned specifically. The mechanism of chromium adsorption from relevant sources with three, four and five parameter models in literature is very limited[40,41]. Hence it is essential to formulate the adsorption phenomena with well-designed models describing adsorption isotherms.

Description with high parameter models may lead to provide very clear and apt information about the adsorption process under equilibrium condition. Then the applicability of one and two parameter isotherm models have very limited[41-44]. The high parameter model would overcome the limitations of the simple models with two-parameter[44-47]. The objectives of the present research were to study the single metal removal efficiency and biosorption capacity of BGMA for the removal of Cr (VI) metal ions from the synthetically prepared stock solution. More emphasis was given to analyze the isotherm data-two, three, four and five parameter models.

MATERIALS AND METHODS

Blue Green Marine Algae (BGMA) used in this investigation to recover the hexavalent chromium metal ion from its respective synthetic solution under equilibrium condition. Preparation of adsorbent, synthetic stock solution and determination optimum experimental parameters viz., pH, temperature and adsorbent dosage under batch condition were provided here along with the effect initial metal ion concentration of equilibrium metal uptake. Analyses of effluent concentration to calculate the equilibrium metal uptake experimentally and theoretically with isotherm models were discussed.

Adsorbent-BGMA: BGA used in this investigation for the study of biosorption of Cr (VI) ions from its synthetic stock solution. The algae were collected from ponds in and around Chidambaram town and Veeranam Lake. The algae was washed with distilled water and dried at room temperature (above 30°C) then it was powdered with a uniform size of 150-200 microns. The dried and powered algae was immobilized on silica gel using standard methods for

continuous adsorption[48] which involves wetting a mixture of silica gel and biomass with ultra pure water followed by drying at 150°C for 20 min.

Adsorbate-Cr (VI): Analytical grade salt Potassium Dichromate $K_2Cr_2O_7$ is used to prepare the synthetic hexavalent chromium Cr (VI) solution. The stock solution of Cr (VI) was prepared by dissolving a pre calculated quantity of respective salt in double distilled water. This stock solutions are further diluted to obtain desired concentration in the range of 25-200 ppm. The pH of each solution is adjusted 2-6. The pH adjustments were done by using 0.1 N nitric acid (HNO_3) and 0.1 N sodium hydroxide (NaOH) solutions.

Analysis: The batch bio sorption study was carried out in a 500 mL conical flask. The initial metal ion concentrations are varied to 25, 50, 100, 125, 150, 175, 200 and 250 ppm. The pH adjustments are done by using 0.1 N nitric acid (HNO_3) and 0.1 N sodium hydroxide (NaOH) solutions. The biomass to be added to the conical flask is varied from 0.5, 1.0, 1.5, 2.0 and 2.5 g. All the experiments are performed at the room temperature. The flasks are kept in a rotary shaker at rpm of 120 for 24 h. This is more than sufficient for adsorption equilibrium. The samples are taken regularly with predetermined time intervals. The percentage removal and specific uptake of metal is then calculated.

The bio sorption of Cr (VI) metal ions from its respective synthetic solutions by the BGMA is performed under shaking conditions in rotary shaker (REMI-12, India). The experiments are performed under batch operation mode. To each 400 mL of metal solution a desired quantity of the blue green microalgae is added in 500 mL conical flasks. The mixture is agitated in the rotary shaker at the room temperature and at 120 rpm for predetermined time intervals.

The initial and final concentrations of metal solutions are predicted by double beam Atomic Adsorption Spectrophotometer (AAS SL176-Elico Limited India). The percentage removal of metal ions is calculated from the initial concentration (C_i) and the analyzed final concentration (C_{eq}) of the metal ion solution according to the following Eq. 1:

$$\text{Removal } (\%) = \frac{C_i - C_{eq}}{C_i} \times 100 \quad (1)$$

The equilibrium metal uptake is calculated from the initial concentration (C_i) and the analyzed final concentration (C_{eq}) of the metal ion solution according to the following Eq. 2:

$$q = \frac{V}{M}\left(C_i - C_{eq}\right) \quad (2)$$

where, V is the volume of liquid sample in liter and M is the weight of bio sorbent. The same procedure is repeated for another initial metal ion concentration of 50, 75, 100, 125, 150, 175, 200 and 250 ppm of all the metals. The experimental variables namely pH and biomass loading are optimized and at these optimized conditions the effect of Initial metal ion concentration on percentage removal and specific uptake of metal ions are studied.

EQUILIBRIUM ADSORPTION ISOTHERMS

Two parameter models (Langmuir, Freundlich, Dubinin-Radushkevich, Temkin, Hill-de Boer, Fowler-Guggenheim, Flory-Huggins, Halsey, Harkin-Jura, Jovanovic and Elovich, Kiselev), Three parameter models (Hill, Redlich-Peterson, Sips, Langmuir-Freundlich, Fritz-Schlunder-III, Radke-Prausnits-I, Radke-Prausnits-II, Radke-Prausnits-III, Toth, Khan, Koble-Corrigan, Jossens, Jovanovic-Freundlich, Brouers-Sotolongo, Vieth-Sladek, Unilan, Holl–Krich and Langmuir–Jovanovic), Four parameter models (Fritz-Schlunder-IV, Baudu Weber-van Vliet and Marczewski-Jaroniec) and Five parameter model (Fritz-Schlunder-5) are used to analyze the experimental equilibrium adsorption data.

Cftool and goodness-of-fit statistics: Applicability of these models to fit the experimental data in predicting the mechanism of adsorption is accomplished using cftool kit available in MATLAB R2010a software. This toolkit aids in estimating the model parameters along with the non-linear Regression coefficient (R^2), Sum of Squares due to Error (SSE) and Root Mean Squared Error (RMSE).

Isotherm models-theoretical knowledge: The isotherms of adsorption indicate the distribution of molecules between the liquid and solid phase when the adsorption process reaches equilibrium. It is employed to establish the maximum capacity of adsorption of metals on adsorbents, expressed in terms of quantity of metal adsorbed per unit mass of adsorbent used (mg g^{-1}). Insight knowledge on adsorption mechanism provides proper understanding and interpretation on the phenomena of adsorption of metal ions on the surface of adsorbents. This enables to improvise the adsorption pathways to facilitate effective design of adsorption[49,50].

Two parameter models: In this section, more attention is paid to accrue theoretical insight knowledge on models containing two parameters to explain the adsorption mechanism. Essential theoretical approach for a total of twelve models

viz., Langmuir, Freundlich, Dubinin-Radushkevich, Temkin, Hill-de Boer, Fowler-Guggenheim, Flory-Huggins, Halsey, Harkin-Jura, Jovanovic, Elovich and Kiselev are provided.

Langmuir isotherm model: The Langmuir model assumes that the surface as homogeneous. This model clearly indicates that the adsorption sites have equal sorbate affinity. Also the adsorption at one site does not affect sorption at the adjacent site. The formation of monolayer coverage of the adsorbate at the outer surface of the adsorbent is well explained by this model. It accounts the surface coverage by balancing the rate of adsorption and rate of desorption relatively under equilibrium condition.

This model sates that the rate of adsorption is proportional to the fraction of the adsorbent surface that is open while desorption is proportional to the fraction of the adsorbent surface that is covered[51,52]. The model is given in Eq. 3:

$$q_{eq} = \frac{q_{max} b_L C_{eq}}{1+b_L C_{eq}} \quad (3)$$

where, b_L is Langmuir constant related to adsorption capacity (mg g^{-1}), which correlates the variation of the suitable area and porosity of the adsorbent. The features of the Langmuir isotherm can be explained by a dimension less constant called the Langmuir separation factor R_L which is calculated as Eq. 4:

$$R_L = \frac{1}{1+b_L q_{max}} \quad (4)$$

where, R_L values indicate the adsorption to be unfavorable when $R_L>1$, linear when $R_L = 1$, favourable when $0<R_L<1$ and irreversible when $R_L = 0$.

Freundlich isotherm model: The Freundlich adsorption isotherm model indicates the extent of heterogeneity of the adsorbent surface. The adsorptive sites are made up of small heterogeneous adsorption sites each of which is homogeneous[28]. The model is given in Eq. 5:

$$q_{eq} = a_F C_{eq}^{\frac{1}{n_F}} \quad (5)$$

where, a_F is Freundlich adsorption capacity (L mg^{-1}) and n_F is adsorption intensity. Relative distribution of the energy and the heterogeneity of the adsorbate sites are well indicated by this model. The larger the value of the adsorption capacity a_F, the higher the adsorption capacity is. The magnitude of $1/n_F$ ranges between 0 and 1, is an indicative of favourable adsorption, becoming more heterogeneous as its value tends to zero[53,54].

Dubinin-radushkevich isotherm model: This empirical model assumes a multilayer character involving Van Der Waal's forces applicable for physical adsorption processes. It is often used to estimate the characteristic porosity in addition to the apparent free energy of adsorption[55]. This empirical model is initially conceived for the adsorption of subcritical vapours onto micro pore solids following a pore filling mechanism. This model provides insight knowledge on the adsorption of gases and vapours on micro porous sorbents[56].

This isotherm is applicable for intermediate range of adsorbate concentrations because it exhibits unrealistic asymptotic behaviour and does not predict Henry's laws at low pressure. Also it is suitable to distinguish the physical and chemical adsorption of metal ions with its mean free energy. Another unique feature of the Dubinin-Radushkevich isotherm is the fact that it is temperature dependent[57,58]. Dubinin-Radushkevich isotherm model is given in Eq. 6:

$$q_{eq} = K_{DR} \exp\left[-B_{DR}\left(RT \ln\left(1+\frac{1}{C_{eq}}\right)\right)^2\right] \quad (6)$$

$$\varepsilon = RT \ln\left[\frac{1}{C_{eq}}\right] \quad (7)$$

where, ε is called as Polanyi Potential shown in Eq. 7. The energy of activation or mean free energy E (kJ mol^{-1}) of adsorption per molecule of the adsorbate when it is transferred to the surface of the solid from infinity in the solution and can be calculated by the Eq. 8.

$$E = \frac{1}{\sqrt{2K_{DR}}} \quad (8)$$

The value of E is used to predict whether an adsorption is physisorption or chemisorptions. If E<8 KJ mol^{-1}, the adsorption is physisorption and if E = 8-16 KJ mol^{-1}, the adsorption is chemisorptions in nature[59].

Temkin isotherm model: Temkin adsorption isotherm model is highly suitable for predicting the gas phase adsorption equilibrium. On the other hand, complex adsorption systems including the liquid-phase adsorption

isotherms are usually not suitable to be described. Moreover, Temkin isotherm model is valid only for an intermediate range of ion concentrations. It illustrates the effects of indirect adsorbate/adsorbate interactions on the adsorption process. The main assumption in this model is the heat of adsorption decreases linearly with increasing coverage and the adsorption is characterized by a uniform distribution of binding energies[60,61]. The Temkin adsorption isotherm model is given in Eq. 9:

$$q_{eq} = \frac{RT}{b_T}\left(\ln A_T C_{eq}\right) \quad (9)$$

The term RT/b_T correlates the heat of adsorption. A_T is the equilibrium binding constant (L mg^{-1}) equivalent to the maximum binding energy.

Hill-de boer isotherm model: Mobile adsorption as well as lateral interaction among adsorbed molecules are well described by this Hill-Deboer isotherm model[62,63]. The Hill-Deboer isotherm model is given in Eq. 10:

$$K_1 C_{eq} = \frac{\theta}{1-\theta}\exp\left(\frac{\theta}{1-\theta} - \frac{K_2\theta}{RT}\right) \quad (10)$$

Positive value of K_2 indicates the attraction between adsorbed species and the negative value of K_2 is the indication of repulsion. If K_2 is equal to zero, it indicates no interaction between adsorbed molecules and it reduces to the Volmer equation[64].

Fowler-guggenheim isotherm model: Fowler-Guggenheim adsorption isotherm model details the lateral interaction of the adsorbed molecules. This is the simplest model allowing for the lateral interaction and it indicates that the heat of adsorption varies linearly with loading. Fowler-Guggenheim adsorption isotherm model is given in Eq. 11:

$$K_{FG} C_{eq} = \frac{\theta}{1-\theta}\exp\left[\frac{2\theta W}{RT}\right] \quad (11)$$

Positive W indicates that the interaction between the adsorbed molecules is attractive. Negative W value is the indication of the interaction among adsorbed molecules is repulsive. If W is equal to zero, there is no interaction between adsorbed molecules and this model reduced to the Langmuir[65,66]. This model simply relates the interaction between the adsorbed molecules and heat of adsorption. If the interaction between the adsorbed molecules is attractive it results an increase in heat of adsorption. Similarly If the interaction between the adsorbed molecules is repulsive, it results a decrease in heat of adsorption.

Flory-huggins isotherm model: Flory-Huggins isotherm discusses the degree of surface coverage characteristics of the adsorbate onto the adsorbent. This model is well appropriate to find the feasibility and spontaneous nature of an adsorption process[40,41,67,68]. Flory-Huggins adsorption isotherm model is given in Eq. 12:

$$\frac{\theta}{C_{in}} = K_{FH}\left[1-\theta\right]^{nFH} \quad (12)$$

where, K_{FH} is used to calculate the spontaneity Gibbs free energy.

Halsey isotherm model: Halsey adsorption isotherm model is appropriate to discuss the multilayer adsorption at a relatively large distance from the surface. The fitting of the experimental data to this equation prove to the heterosporous nature of the adsorbent[69]. Halsey adsorption isotherm model is given in Eq. 13:

$$q_{eq} = \text{Exp}\left[\frac{\text{Ln}\,K_{Ha} - \text{Ln}\,C_{eq}}{n_{Ha}}\right] \quad (13)$$

Harkin-jura isotherm model: Hurkin-Jura adsorption isotherm accounts for multilayer adsorption on the surface of absorbents having heterogeneous pore distribution. The existence of a heterogeneous pore distribution can be well explained by this model[25]. Hurkin-Jura adsorption isotherm model is given in Eq. 14:

$$q_{eq} = \sqrt{\frac{A_{HJ}}{B_{HJ} - \text{Log}\,C_{eq}}} \quad (14)$$

Jovanovic isotherm model: Jovanovic adsorption isotherm model is similar to that of Langmuir model with the approximation of monolayer localized adsorption without lateral interactions. The assumptions in this model are same in the Langmuir model in addition with the possibility of some mechanical contacts between the adsorption and desorbing molecules[70]. Jovanovic adsorption isotherm model is given in Eq. 15:

$$q_{eq} = q_{max}\left[1 - e^{-\left(K_J C_{eq}\right)}\right] \quad (15)$$

At high concentrations of adsorbate, it becomes the Langmuir isotherm, however does not follow the Henry's law.

Elovich isotherm model: The Elovich isotherm model assumes that the adsorption site grows exponentially with adsorption, indicating a multilayer adsorption. It is highly useful in describing chemisorption on highly heterogeneous adsorbents. This model is often valid for systems in which the adsorbing surface is heterogeneous[71]. The Elovich adsorption isotherm model is given in Eq. 16:

$$\frac{q_{eq}}{q_{max}} = K_E C_{eq} \exp^{\frac{q_{eq}}{q_{max}}} \quad (16)$$

Kiselev isotherm model: The Kiselev adsorption isotherm model explains the localized monomolecular layer formation of adsorbate on adsorbents[72]. This model is valid when surface coverage is greater than 0.68. The Kiselev adsorption isotherm model is given in Eq. 17:

$$K_{eqK} C_{eq} = \frac{\theta}{(1-\theta)(1+K_{nK}\theta)} \quad (17)$$

Three parameter models: Models containing three parameters to explain the mechanism of adsorption are discussed using sixteen models viz., Hill, Redlich-Peterson, Sips, Langmuir-Freundlich, Fritz-Schlunder-III, Radke-Prausnits, Toth, Khan, Koble-Corrigan, Jossens, Jovanovic-Freundlich, Brouers-Sotolongo, Vieth-Sladek, Unilan, Holl-Krich and Langmuir-Jovanovic.

Hill isotherm model: The Hill isotherm model is derived to describe the adherence of different species onto homogeneous substrates. An assumption is made in this model is adsorption is a cooperative phenomena. It indicates that the adsorbate at one site of the adsorbent would influence the other sites on the same adsorbent[73]. Hill adsorption isotherm model is given in Eq. 18:

$$q_{eq} = \frac{q_{max} C_{eq}^{nH}}{K_H + C_{eq}^{nH}} \quad (18)$$

If n_H is greater than 1, this isotherm indicates positive co-operativity in binding, n_H is equal to 1, it indicates non-cooperative or hyperbolic binding and n_H is less than 1, indicating negative co-operativity in binding.

Redlich-peterson isotherm model: The Redlich-Peterson isotherm model is derived with hybrid features of Langmuir and Freundlich isotherms. Consequently the mechanism of adsorption is a hybrid one and it does not follow ideal monolayer adsorption[74]. This Redlich-Peterson isotherm model is given in Eq. 19:

$$q_{eq} = \frac{A_{RP} C_{eq}}{1 + B_{RP} C_{eq}^{\beta}} \quad (19)$$

This model is applicable with wide concentration range, the model has a linear dependence on concentration in the numerator and an exponential function in the denominator. It is applicable for both homogeneous and heterogeneous systems. At high liquid-phase concentrations of the adsorbate, Redlich-Peterson isotherm model reduces to the Freundlich model. This model approaches Henrys Law model when the liquid phase concentration is low. The exponent, β_{RP}, generally ranges between 0 and 1. While $\beta_{RP} = 1$ this model approaches Langmuir model and $\beta_{RP} = 0$ this isotherm approaches to Freundlich model.

Sips isotherm model: Sips adsorption isotherm model described mainly the localized adsorption without adsorbate-adsorbate interactions[75]. This model is a combined of Langmuir and Freundlich expressions developed to predict the heterogeneous adsorption systems. The limitation of increased adsorbate concentration normally associated with the Freundlich isotherm is neglected in this model. At low adsorbate concentrations, it is transformed to Freundlich isotherm. At high adsorbate concentrations, it predicts a monolayer adsorption capacity characteristic of the Langmuir isotherm[76]. Sips adsorption isotherm model is given in Eq. 20:

$$q_{eq} = \frac{q_m K_s C_{eq}^{\beta s}}{1 + K_s C_{eq}^{\beta s}} \quad (20)$$

When β_S equal to 1 this isotherm approaches Langmuir isotherm and β_S equal to 0, this isotherm approaches Freundlich isotherm.

Langmuir-freundlich isotherm model: Langmuir-Freundlich isotherm model describes the adsorption in heterogeneous surfaces. It explains the distribution of adsorption energy of the adsorbent onto heterogeneous surface. When the adsorbate concentration is low, this model becomes the Freundlich isotherm model, contradictorily when the adsorbate concentration is high, this model becomes the Langmuir isotherm[51]. Langmuir-Freundlich isotherm model is given in Eq. 21:

$$q_{eq} = \frac{q_{max} \left(K_{LF} C_{eq}\right)^{m_{LF}}}{1 + \left(K_{LF} C_{eq}\right)^{m_{LF}}} \quad (21)$$

where, m_{LF} is heterogeneous parameter and it lies between 0 and 1. m_{LF} would increase with a decrease in degree of surface heterogeneity. For mLF is equal to 1, this model covert to Langmuir model.

Fritz-schlunder-III isotherm model: Fritz-Schlunder three parameter isotherm models is developed to fit over an extensive range of experimental results because of huge number of coefficients in their isotherm[77]. This expression is given in Eq. 22:

$$q_{eq} = \frac{q_{max} K_{FS3} C_{eq}}{1+q_{max} C_{eq}^{m_{FS3}}} \quad (22)$$

If m_{FS3} is equal to 1, the Fritz–Schlunder–III model becomes the Langmuir model but for high concentrations of adsorbate, the Fritz–Schlunder–III reduces to the Freundlich model.

Radke-prausnitz isotherm model: The Radke-Prausnitz isotherm model has several important properties which makes it more preferred in most adsorption systems at low adsorbate concentration. This isotherm is applicable over a wide range of adsorbate concentration. This isotherm model reduces to a linear isotherm (Henrys Model) when the adsorbate concentration is low. This model becomes the Freundlich isotherm when the adsorbate concentration is high. When Radke-Prausnitz model exponent m_{RaP3} is equal to zero, this model becomes the Langmuir isotherm[78]. Radke-Prausnitz isotherm models are given in Eq. 23-25:

$$\text{Model 1} \quad q_{eq} = \frac{q_{max} K_{RaP1} C_{eq}}{\left[1+K_{RP1} C_{eq}\right]^{m_{RaP1}}} \quad (23)$$

$$\text{Model 2} \quad q_{eq} = \frac{q_{max} K_{RaP2} C_{eq}}{1+K_{RP2} C_{eq}^{m_{RaP2}}} \quad (24)$$

$$\text{Model 3} \quad q_{eq} = \frac{q_{max} K_{RaP3} C_{eq}^{m_{RaP3}}}{1+K_{RP3} C_{eq}^{m_{RaP3-1}}} \quad (25)$$

If the value of both m_{RaP1} and m_{RaP2} is equal to 1, the Radke-Prausnitz 1, 2 models reduce to the Langmuir model but at low concentrations, the models become Henry's law, but for high adsorbate concentration, the Radke-Prausnitz 1 and 2 models becomes the Freundlich model. But the Radke-Prausnitz-3 equation reduces to Henry's law while the exponent m_{RaP3} is equal to 1 and become Langmuir isotherm when the exponent m_{RaP3} is equal to 0.

Toth isotherm model: Toth adsorption isotherm model is developed to describe the heterogeneous adsorption systems which satisfy both low and high end boundary of adsorbate concentration. This model is the modified form of Langmuir isotherm with the intension of rectifying the error between experimental and predicted data[79]. The Toth isotherm model is given Eq. 26:

$$q_{eq} = \frac{q_{max} C_{eq}}{\left(\frac{1}{K_T}+C_{eq}^{n_T}\right)^{\frac{1}{n_T}}} \quad (26)$$

It is clear that when n = 1, this equation reduces to Langmuir isotherm equation, the process approaches onto the homogeneous surface. Therefore the parameter n characterizes the heterogeneity of the adsorption system. If it deviates further away from unity, then the system is said to be heterogeneous. This isotherm model is suitable for the modelling of several multilayer and heterogeneous adsorption systems.

Khan isotherm model: The Kahn isotherm model is developed for adsorption of bi-adsorbate from pure dilute equations solutions. This isotherm has applicable on both limits Freundlich on one end and Langmuir isotherm on the other end[80]. Kahn isotherm model is given in Eq. 27:

$$q_{eq} = \frac{q_m b_K C_{eq}}{\left(1+b_K C_{eq}\right)^{aK}} \quad (27)$$

While, a_K is equal to 1, Toth model approaches the Langmuir isotherm model and at higher values of concentration, Toth model reduces to the Freundlich isotherm model.

Koble-corrigan isotherm model: Koble-Corrigan isotherm model is the resemblance of Sips isotherm model. This model incorporates both Langmuir and Freundlich isotherm[81]. Koble-Corrigan isotherm model is given in Eq. 28:

$$q_{eq} = \frac{A_{KC} C_{eq}^{n_{KC}}}{1+B_{KC} C_{eq}^{n_{KC}}} \quad (28)$$

This model reduces to Freundlich at high adsorbate concentrations. It is only valid when the constant n is greater than or equal to 1. When n is less than unity, it signifies that the model is incapable of defining the experimental data despite high concentration coefficient or low error value.

Jossens isotherm model: The Jossens isotherm model is developed on the basis of energy distribution of adsorbate-adsorbent interactions at adsorption sites. An assumption is made in this model is the adsorbent has heterogeneous surface with respect to the interactions it has with the adsorbate[82]. At low concentrations this model is reduced to Henry's law model. Jossens isotherm model is given in Eq. 29:

$$q_{eq} = \frac{K_J C_{eq}}{1 + J C_{eq}^{bJ}} \quad (29)$$

where, J is corresponds to Henry's constant at low capacities. b_J is Jossens isotherm constant and it is characteristic of the adsorbent irrespective of temperature and the nature of adsorbents.

Jovanovic freundlich isotherm model: Jovanovic-Freundlich isotherm model is developed to describe single-component adsorption equilibrium on heterogeneous surfaces. An assumption is made in this model is the rate of decrease of the fraction of the surface unoccupied by the adsorbate molecules is proportional to a certain power of the partial pressure of the adsorbate. If the adsorbent surface is homogeneous, this model reduced to Jovanovic. At low pressures, the equation reduces to the Freundlich isotherm but at high pressures, monolayer coverage is achieved. As in the case of Jovanovic model, the Jovanovic-Freundlich model regard as the possibility of some mechanical contacts between the adsorbing and desorbing molecules. Furthermore, this isotherm was utilized for heterogeneous surfaces without lateral interactions[83]. Jovanovic-Freundlich isotherm model is given in Eq. 30:

$$q_{eq} = q_{max}\left[1 - e^{-\left(K_{JF} C_{eq}^{nJF}\right)}\right] \quad (30)$$

Brouers-sotolongo isotherm model: This isotherm is designed in the form of deformed exponential function for adsorption onto the heterogeneous surface mainly because of Langmuir who has recommended the extension of the simple Langmuir isotherm to non-uniform adsorbent surfaces. The assumption made in this isotherm is the surface of adsorbent consists of a fixed number of patches of active sites of equal energy[84]. Brouers-Sotolongo model is given in Eq. 31:

$$q_{eq} = q_{max}\left[1 - e^{\left(-K_{BS} C_{eq}^{\alpha BS}\right)}\right] \quad (31)$$

The parameter a_{BS} is related with distribution of adsorption energy and the energy of heterogeneity of the adsorbent surfaces at the given temperature[85].

Vieth-sladek isotherm model: This model incorporates two distinct sections to calculate the diffusion rates in solid adsorbents from transient adsorption. The first one is defined by a linear section (Henry's law) and second one is non-linear section (Langmuir isotherm). The linear section clarifies the physisorption of gas molecules onto the amorphous adsorbent surfaces and the non-linear section explains the adherence of gas molecules to sites on the porous adsorbent surfaces[86]. Vieth-Sladek isotherm model is given in Eq. 32:

$$q_{eq} = K_{VS} C_{eq} + \frac{q_{max} \beta_{VS} C_{eq}}{1 + \beta_{VS} C_{eq}} \quad (32)$$

Unilan isotherm model: Unilan isotherm model is presumed the application of the local Langmuir isotherm and uniform energy distribution. This equation is restricted to Henry's law, thus it is valid at extremely low adsorbate concentrations. It is frequently used for adsorption of gas phase onto a heterogeneous adsorbent surface[76]. Unilan isotherm model is given in Eq. 33:

$$q_{eq} = \frac{q_{max}}{2\beta_U} Ln\left[\frac{1 + K_U C_{eq} e^{\beta U}}{1 + K_U C_{eq} e^{-\beta U}}\right] \quad (33)$$

The higher the model exponent β_U, the system is more heterogeneous. If β_U is equal to 0, the Unilan isotherm model becomes the classical Langmuir model as the range of energy distribution is zero in this limit[82,87,88].

Holl-krich isotherm model: Holl-Krich Isotherm Model is a modified form of Langmuir isotherm[89]. This model becomes the Freundlich isotherm at low concentrations. The capacity reaches a finite capacity more leisurely than the Langmuir isotherm at high concentrations[55]. Holl-Krich Isotherm Model is given in Eq. 34:

$$q_{eq} = \frac{q_{max} K_{HK} C_{eq}^{n_{HK}}}{1 + K_{HK} C_{eq}^{n_{HK}}} \quad (34)$$

Langmuir-jovanovic isotherm model: This empirical model is the combined form of both Langmuir and Jovanovic isotherm[90]. The Langmuir-Jovanovic model is given in Eq. 35:

$$q_{eq} = \frac{q_{max} C_{eq}\left[1 - e^{\left(K_{LJ} C_{eq}^{nLJ}\right)}\right]}{1 + C_{eq}} \quad (35)$$

Four parameter models: The four parameter models discussed in this study are Fritz-Schlunder-IV, Baudu, Weber-van Vliet and Marczewski-Jaroniec models.

Fritz-schlunder-IV isotherm model: Fritz-Schlunder IV model is another model comprised of four-parameter with combine features of Langmuir-Freundlich isotherm[77]. The model is given in Eq. 36:

$$q_{eq} = \frac{A_{FS5} C_{eq}^{\alpha_{FS5}}}{1 + B_{FS5} C_{eq}^{\beta_{FS5}}} \quad (36)$$

This isotherm is valid when the values of α_{FS5} and β_{FS5} are less than or equal to 1. At high adsorbate concentration, Fritz-Schlunder-IV isotherm becomes Freundlich equation. Conversely if the value of both a_{FS5} and β_{FS5} equal to 1, this isotherm reduces to Langmuir isotherm. At high concentrations of the adsorbate in the liquid-phase this isotherm model becomes the Freundlich.

Baudu isotherm model: Baudu isotherm model has been developed mainly due to the arise of discrepancy in calculating Langmuir constant and coefficient from slope an tangent over a broad range of concentrations[91]. Baudu isotherm model is the transformed form of the Langmuir isotherm. It is given in Eq. 37:

$$q_{eq} = \frac{q_{max\ bo} C_{eq}^{(1+x+y)}}{1 + b_o C_{eq}^{(1+x)}} \quad (37)$$

This model is only applicable in the range of (1+x+y)<1 and (1+x)<1. For lower surface coverage, Baudu model reduces to the Freundlich equation[92]. It is given in Eq. 38:

$$q_{eq} = \frac{q_{mo\ bo} C_{eq}^{(1+x+y)}}{1 + b_o} \quad (38)$$

Weber-van vliet isotherm model: Weber and van Vliet isotherm model is to describe equilibrium adsorption data with four parameters[93,94]. The model is given in Eq. 39:

$$C_{eq} = P_1 q_{eq}^{\left(P_2 q_{eq}^{P3} + P4\right)} \quad (39)$$

The isotherm parameters P_1, P_2, P_3 and P_4 can be defined by multiple nonlinear curve fitting techniques which is predicated on the minimization of sum of square of residual.

Marczewski-jaroniec isotherm model: The Marczewski-Jaroniec isotherm model is the resemblance of Langmuir isotherm model. It is developed on the basis of the supposition of local Langmuir isotherm and adsorption energies distribution in the active sites on adsorbent[89,94]. The Marczewski-Jaroniec isotherm model is given in Eq. 40:

$$q_{eq} = q_{max}\left[\frac{\left(K_{MJ} C_{eq}\right)^{n_{MJ}}}{1 + \left(K_{MJ} C_{eq}\right)^{n_{MJ}}}\right] \quad (40)$$

where, K_{MJ} describes the spreading of distribution in the path of higher adsorption energy. n_{MJ} describes the spreading in the path of lesser adsorption energies. The isotherm reduces to Langmuir isotherm when n_{MJ} and K_{MJ} are equal to unity. The isotherm reduces to Langmuir-Freundlich model when n_{MJ} equal to KMJ.

Five parameter model: Accounting the high parameter models certainly provides clear information on mechanism of adsorption under equilibrium condition. In this section, only one, five parameter model i.e., Fritz-Schlunder-V isotherm model is applied.

Fritz-schlunder-V isotherm model: Fritz-Schlunder adsorption isotherm model is developed with the aim of simulating the model variations more precisely for application over a wide range of equilibrium data[77]. Fritz-Schlunder adsorption isotherm model is given in Eq. 41:

$$q_{eq} = \frac{q_{max} K_{1FS5} C_{eq}^{\alpha_{FS5}}}{1 + K_{2FS5} C_{eq}^{\beta_{FS5}}} \quad (41)$$

RESULTS AND DISCUSSION

Experimental results show that the maximum adsorption of Cr (VI) by BGMA can be achieved at pH of 5 and at 2 g of BGMA biomass loading. The maximum adsorption capacity of BGMA is found to be 37.426 mg g^{-1}. The optimum agitation rate 120 rpm is maintained during the continuous 24 h of contact time.

To validate the prediction of maximum adsorption capacity of BGMA, the finding is compared with several authors who have reported their results of the investigation on adsorption of Cr (VI) using different sorbents. The maximum adsorption capacity of activated charcoal (prepared from wood apple shell) used by Doke and Khan[95] for removal of Cr (VI) from aqueous solution of concentration 1250 mg g^{-1} is reported to be 151.51 mg g^{-1} at a pH 1.8. Though the q_{max} is relatively very higher than the present investigation, their

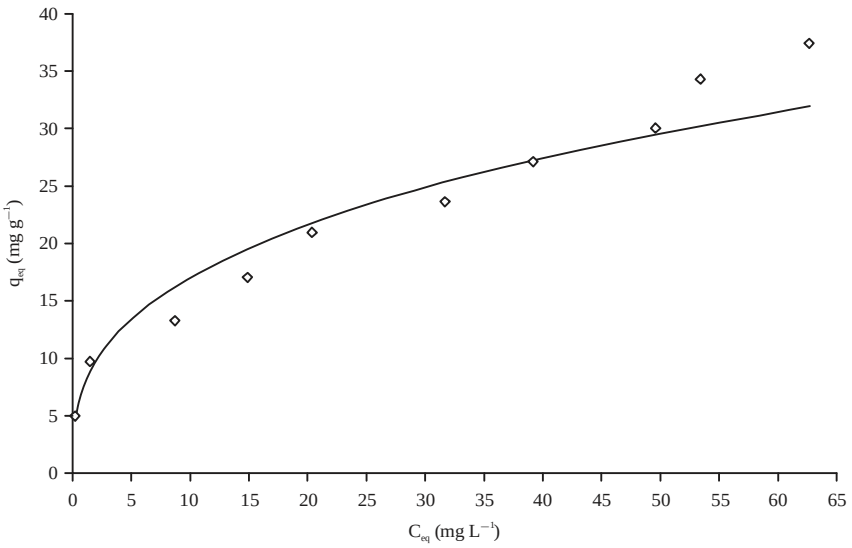

Fig. 1: Experimental results of adsorption of Cr (VI) onto BGMA

sorbent are found to be more effective at a low pH which is highly acidic. However such acidic environments are tedious, hazardous and also uneconomical to industrial scale. Similarly a new low-cost activated carbon is prepared by Gorzin and Abadi[96] from paper mill sludge in order to remove Cr (VI) ions from aqueous solution of concentration 100 mg L^{-1}. The maximum adsorption capacity of 23.18 mg g^{-1} is reported at optimum pH 4.0 and contact time of 180 min. Subsequently magnetic natural zeolite-Chitosan composite is used as adsorbent to remove Cr (VI) from an aqueous solution of 200 mg L^{-1} concentration by Gaffer *et al.*[97]. The 98% of removal efficiency is reported at pH 2 and 0.2 g of dosage. Chemically treated banana peels is used by Ali *et al.*[98] as an adsorbent for removal of Cr (VI) from aqueous solution of concentration 400 mg L^{-1} and the maximum adsorption capacity reported is reported to be 6.178 mg g^{-1} at 120 min contact time, 4.0 g L^{-1} adsorbent dosage and 3.0 pH. Potato peels is used by Mutongo *et al.*[99] as adsorbent for removal of Cr (VI) from aqueous solution of concentration 100 mg L^{-1} and the maximum adsorption capacity is reported as 3.28 mg g^{-1} at 48 min contact time, 4.0 g L^{-1} adsorbent dose and 2.5 pH. Mulani *et al.*[100] studied the removal of chromium (VI) was performed using coffee polyphenol-formaldehyde/acetaldehyde resins as adsorbent. The maximum adsorption capacity of coffee polyphenol-formaldehyde resins is reported as 19.342 mg g^{-1} at pH 2 and 150 min contact time.

Contradictorily, Guar gum–nano zinc oxide (GG/n ZnO) bio composite is used as an adsorbent by Khan *et al.*[101] for enhanced removal of Cr (VI) from aqueous solution of concentration 25 mg L^{-1} and the maximum adsorption capacity is reported as 55.56 mg g^{-1} at 50 min contact time, 1.0 g L^{-1} adsorbent dose and 7.0 pH. Though the reported q_{max} is found to be very high efficiency with an artificially made sorbent, this is comparatively inferior to naturally occurring BGMA in terms of availability, accessibility and cost.

Adsorption isotherms: The shape of the adsorption isotherms aids to classify the nature of the phenomena of adsorption of Cr (VI) onto BGMA. The experimental adsorption nature of Cr (VI) from its synthetic aqueous solutions onto BGMA is shown in Fig. 1 which is very much useful to perceive the shape of the isotherm[102,41]. Giles *et al.*[103] classified the isotherms according to their shapes and grouped as L, S, H and C. Based on the above classification, the isotherm of Cr (VI) onto BGMA shows the L curve pattern. The L shape is the indication of no strong competition between solvent and the adsorbate to occupy the adsorbent surface sites. Figure 1 shows concavity curve which indicates that the ratio between the concentration of the compound remaining in solution and adsorbed on the solid decreases when the solute concentration increases. It reveals the progressive saturation of the solid.

Limousin *et al.*[46] details further, two sub-groups of L shaped isotherms: (i) The curve reaches a strict asymptotic plateau (the solid has a limited sorption capacity) and (ii) The curve does not reach any plateau (the solid does not show clearly a limited sorption capacity). Figure 1 infers that BGMA has a limited sorption capacity for adsorption of Cr (VI) under the conditions employed in this investigation.

Two parameter models: The values of parameters and regression coefficient R^2 of two parameter adsorption isotherm models for adsorption of Cr (VI) onto BGMA are

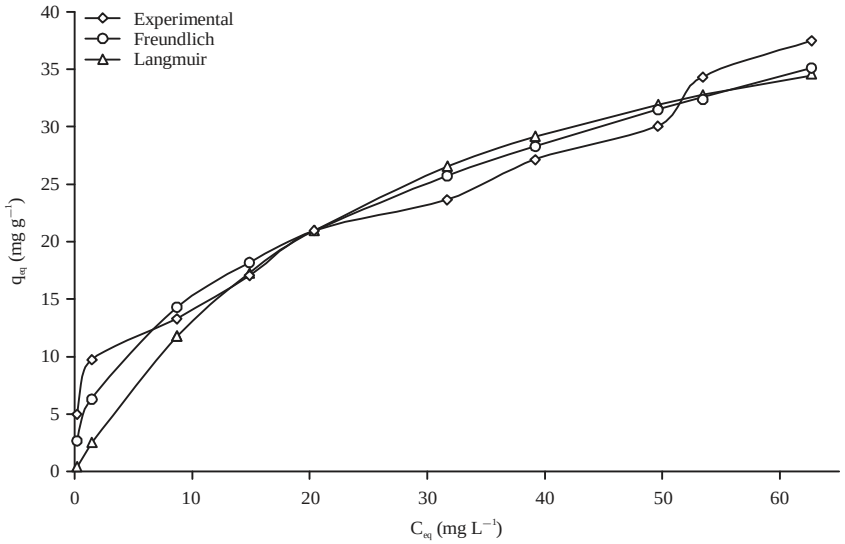

Fig. 2: Comparison of experimental values of equilibrium uptake of Cr (VI) with two parameter model values

Table 1: Parameter values of two parameter adsorption isotherm models for adsorption of Cr (VI) onto BGMA

Models	Parameter	Value	SSE	R^2	RMSE
Langmuir isotherm model	b_L	0.0354	100.9	0.9019	3.552
	q_{max}	50.04			
	R_L	0.3608			
Freundlich isotherm model	a_F (mg g^{-1})	5.315	34.76	0.9662	2.084
	n_F	2.194			
Dubinin-radushkevich model	B_{DR}	7.416×10^{-7}	477.8	0.5358	7.728
	K_{DR}	25.98			
Temkin model	A_T	4.546	191.5	0.8139	4.893
	b_T	474			
Hill-de boer model	K_1	3.375×10^{4}	1.72×10^{13}	-3.795×10^{9}	-1.466×10^{6}
	K_2	2.206×10^{5}			
Fowler-guggenheim model	K_{FG}	1.343×10^{-6}	3121	0.3116	19.75
	W	-1.836×10^{4}			
Flory-huggins isotherm	K_{FH}	0.006463	7.156×10^{4}	-0.3878	94.58
	n_{FH}	2085			
Halsey isotherm model	K_{Ha}	1.287×10^{4}	4067	-2.952	22.55
	n_{Ha}	3.495			
Harkin-jura isotherm model	A_{HJ}	2.576	23	-3.13	32
	B_{HJ}	3.754			
Jovanovic isotherm model	K_J	0.03826	115.5	0.8877	3.8
	q_{max}	37.85			
Elovich isotherm model	K_E	-5.892	5804	-4.64	26.94
	q_{max}	-1			
Kiselev isotherm model	K_{eqK}	-10	4797	-0.05829	24.49
	K_{nK}	-1.341			

given in Table 1. Dubinin-Radushkevich, Hill-de Boer, Fowler-Guggenheim, Flory-Huggins, Halsey, Harkin-Jura, Elovich and Kiselev are eliminated from the running discussion in the initial stage itself due to the negative R-square values. Jovanovic and Temkin are also removed from the discussion due to their low R^2 value when compared to other isotherm models under study. Only two models viz. Freundlich and Langmuir are taken into consideration for further discussion. A plot of C_{eq} (mg L^{-1}) against q_{eq} (mg g^{-1}) for both the models along with experiential values is shown in Fig. 2. Among the two models, Freundlich isotherm model shows greater accuracy with experimental data ($R^2 = 0.9662$). It indicates that the extent of heterogeneity of the BGMA surface. Due to this, the adsorptive surfaces of BGMA are expected to be made up of small heterogeneous adsorption sites that are homogeneous in themselves. Through the surface exchange mechanism, adsorption sites are activated which results in increased adsorption. The value of a_F and n_F are found to be 5.315 mg g^{-1} and 2.194, respectively. Since the value of n_F is in the range of 1-10, it infers that the adsorption of Cr (VI) from

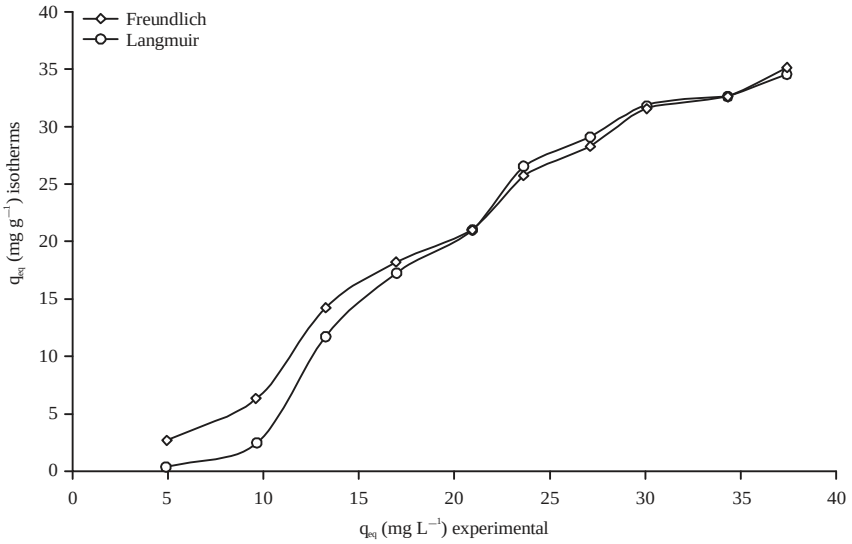

Fig. 3: Accuracy of two parameter model values of equilibrium uptake of Cr (VI) with experimental values

its synthetic solution onto BGMA is favourable one. The value of $1/n_F$ is calculated as 0.4558 which is closer to zero ensures that the active sites of BGMA for adsorption of Cr (VI) onto its surface are more heterogeneous.

Followed by the Freundlich, Langmuir isotherm model shows better agreement with experimental adsorption data with an R^2 value of 0.9019. It suggests the applicability of the Langmuir adsorption isotherm and indicates the formations of monolayer coverage of the sorbate at the outer surface of the sorbent. The value of Langmuir adsorption equilibrium constant b_L is 0.0354 mL g^{-1} which shows quantitatively the affinity between Cr (VI) and BGMA. Since the calculated value of R_L is equal to 0.3608, which is in between 0-1, it ensures that the adsorption of Cr (VI) onto BGMA is favourable. Based on Langmuir isotherm model, the maximum adsorption capacity of BGMA for Cr (VI) is found to be 50.04 mg g^{-1} and it indicates the reasonable agreement of Langmuir isotherm model with experimental data of Cr (VI) adsorption by BGMA form its synthetic solution under the conditions employed in this investigation.

Since the R^2 values of both the Freundlich and Langmuir are highly significant and gives good agreement with the experimental data mathematically, It is suppose to be arrived two different opinions: One is surface heterogeneity of adsorbent through Freundlich isotherm and the another is monolayer coverage of adsorbate onto the surface of adsorbent from Langmuir isotherm. Figure 3 ensures the same and shows the comparison and extent of concurrence of both models with experimental equilibrium uptake.

However it cannot be claimed that both the mechanisms suit for adsorption of Cr (VI) onto BGMA for the entire range of concentration employed in this investigation. From Fig. 4, it is clearly observed that the concurrence of Langmuir isotherm mechanism is lesser than Freundlich when the initial concentration of Cr (VI) synthetic solution is low. Subsequently as the initial concentration is increased to a level of 100 mg L^{-1}, the mechanism shows a closer association with experimental data under equilibrium condition. This trend continuous up to the initial concentration of 120 mg L^{-1}, thereafter the trend deviates from the concurrence. Again in-between 200-220 mg L^{-1} initial concentration level a closer association is noticed. Up to 70 mg L^{-1} and above 220 mg L^{-1} of initial concentration level, though the Freundlich adsorption mechanism shows a deviation from experimental data under equilibrium condition, the magnitude of deviation is less when compared with Langmuir mechanism. Not only that, in-between 70-220 mg L^{-1} initial concentration level is a closer association observed with Freundlich isotherm mechanism than Langmuir. Freundlich isotherm mechanism provides maximum satisfaction with the equilibrium experimental data under the range of experimental conditions investigated in this study.

Three parameter models: Table 2 provides the parameter values for three parameter adsorption isotherm models for adsorption of Cr (VI) onto BGMA. As in the case of two parameter models, Langmuir-Freundlich, Jossens, Jovanovic-Freundlich, Redlich-Peterson Isotherm Model, Radke-Prausnits isotherm Model-II and Toth isotherm model are eliminated from the running discussion in the initial stage itself due to its poor R^2 values. Though Unilan, Hill, Sips, Fritz-Schlunder-III, Radke-Prausnits-I, Khan,

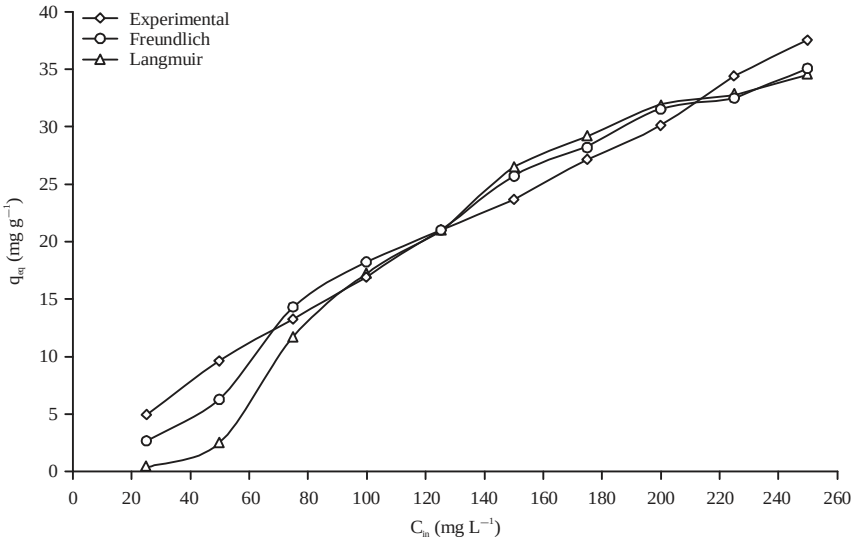

Fig. 4: Concurrence of experimental values of equilibrium uptake of Cr (VI) with two parameter model values upon initial metal ion concentration

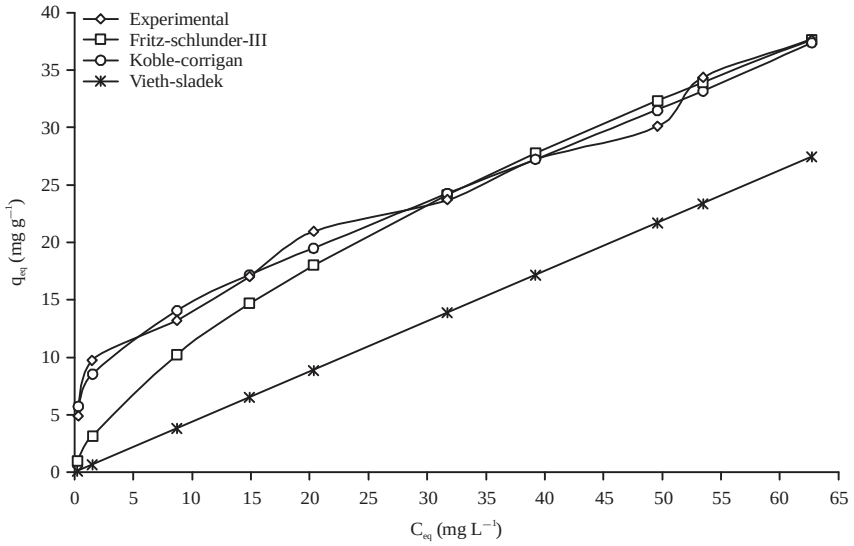

Fig. 5: Comparison of experimental values of equilibrium uptake of Cr (VI) with three parameter model values

Brouers-Sotolongo, Holl-Krich, Langmuir-Jovanovic Isotherm Models have significant R^2 values, the qmax values obtained in each of these models are either negative or too high which are not physically realizable. Hence these models are eliminated from the running discussion.

Koble-Corrigan isotherm Model shows an amazing concurrence with experimental data points. Its R^2 value is equal to 0.9919. Since the value of Koble-Corrigan's isotherm constant (n_{KC} = 0.07927), it signifies that the model is incapable of defining the experimental data despite high concentration coefficient and low error value. Among the eighteen, three parameter models, only two models viz., Vieth-Sladek and Radke-Prausnits-III are taken into the consideration for the running discussion. Figure 5 shows the plot of C_{eq} (mg L^{-1}) against q_{eq} (mg g^{-1}) for the two models along with experiential values. Vieth-Sladek isotherm model gives R^2 value of 0.9652. Hence it is arrived that the adsorption of Cr (VI) onto BGMA is influenced both by van der waals forces (physical adsorption) and ionic forces (chemical adsorption) for the entire range of concentration employed in this investigation. However a conflict of interest is arises upon the lower qmax value of 10.02 mg g^{-1}.

Table 2: Parameter values of three parameter adsorption isotherm models for adsorption of Cr (VI) onto BGMA

Models	Parameter	Value	SSE	R^2	Adj R^2	RMSE
Hill isotherm model	K_H	1596	57.01	0.9446	0.9288	2.854
	n_H	0.3538				
	q_{max}	1.241×10^4				
Redlich-peterson isotherm model	A_{RP}	1.332×10^4	114.50	0.8888	0.857	4.044
	B_{RP}	6687				
	β	0.286				
Sips isotherm model	K_S	0.001247	39.77	0.9614	0.9503	2.384
	q_{max}	5121				
	β	0.4066				
Langmuir-freundlich model	K_{LF}	116.8	813.50	0.2096	-0.0163	10.78
	m_{LF}	0.302				
	q_{max}	23.43				
Fritz-schlunder-III isotherm model	K_{FS3}	2.455	87.97	0.9145	0.8901	3.545
	M_{FS3}	0.34				
	q_{max}	6783				
Radke-prausnits isotherm model-I	K_{RaP1}	19.84	81.86	0.9205	0.8977	3.42
	M_{RaP1}	0.3589				
	q_{max}	0.3861				
Radke-prausnits isotherm model-II	K_{RaP2}	3249	176.40	0.8286	0.7797	5.019
	M_{RaP2}	0.1776				
	q_{max}	1.314				
Radke-prausnits isotherm model-III	K_{RaP3}	0.02039	81.80	0.9205	0.8978	3.418
	M_{RaP3}	0.6439				
	q_{max}	130.6				
Toth isotherm model	K_T	3.014	166.40	0.8383	0.7921	4.876
	n_T	0.03382				
	q_{max}	5.44×10^4				
Khan isotherm model	a_K	0.3615	78.18	0.924	0.9023	3.342
	b_K	288.9				
	q_{max}	0.07209				
Koble-corrigan isotherm model	A_{KC}	2.755	8.365	0.9919	0.9896	1.093
	B_{KC}	-0.6465				
	n_{KC}	0.07927				
Jossens isotherm Model	b_J	0.0321	274.10	0.7337	0.6576	6.257
	J	8069				
	K_J	5976				
Jovanovic-freundlich isotherm model	K_{JF}	9.556	711.90	0.3083	0.1107	10.08
	n_{JF}	2.524				
	q_{max}	23.73				
Brouers-sotolongo isotherm model	K_{BS}	0.004147	39.80	0.9613	0.9503	2.384
	a_{BS}	0.4084				
	q_{max}	1536				
Vieth-sladek isotherm model	K_{VS}	0.437	35.81	0.9652	0.9553	2.262
	β_{VS}	-1.015×10^4				
	q_{max}	10.02				
Unilan isotherm model	K_U	26.48	17.52	0.983	0.9781	1.582
	β_U	-4.893				
	q_{max}	-0.004235				
Holl-krich isotherm model	K_{HK}	0.001655	44.81	0.9565	0.9440	2.53
	n_{HK}	0.3864				
	q_{max}	4154				
Langmuir-jovanovic isotherm model	K_{LJ}	-0.01276	71.80	0.9302	0.9103	3.203
	n_{LJ}	0.3741				
	q_{max}	592.8				

Finally The Radke-Prausnits-III isotherm model gives an appreciable R^2 value of 0.9205. The value of m_{RaP3} is equal to 0.6439 indicates that both Langmuir and Freundlich mechanisms are suitable to describe the adsorption of Cr (VI)

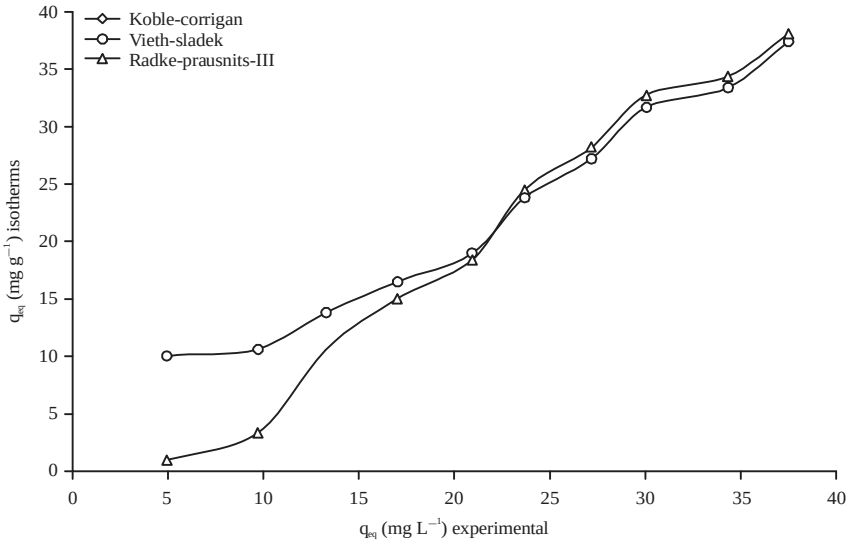

Fig. 6: Accuracy of three parameter model values of equilibrium uptake of Cr (VI) with experimental values

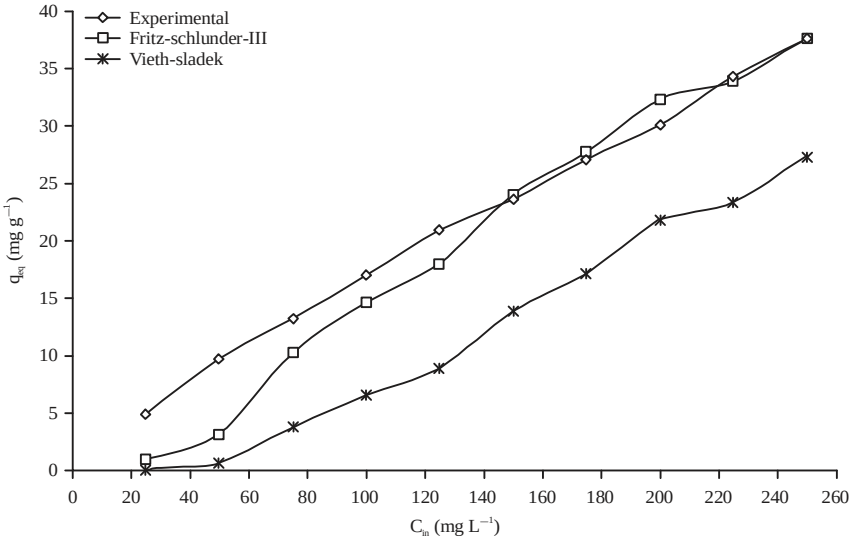

Fig. 7: Concurrence of experimental values of equilibrium uptake of Cr (VI) with three parameter model values upon initial metal ion concentration

onto BGMA for the entire range of concentration employed in this investigation. As in the case of discussion in two parameter model, Radke-Prausnits-III isotherm model ensures this conclusion. Figure 6 shows the comparison and extent of concurrence of three models with experimental equilibrium uptake. Figure 7 is the indication of equilibrium uptake of metal by isotherm models upon the increase in initial concentration of Cr (VI) synthetic solution.

Four parameter models: Fritz-Schlunder-IV Isotherm Model, Baudu Isotherm Model, Weber-van Vliet Isotherm Model and Marczewski-Jaroniec Isotherm Model are investigated to know the mechanism of adsorption of Cr(VI) form its synthetic solution by BGMA. Among the four models, Weber-van Vliet Isotherm Model alone seems to be highly significant (R^2 = 0.9811). Rest of the three models are not applicable due its poor R^2 values and irreverent parameter values. Hence it can describe the mechanism of adsorption of Cr (VI) onto BGMA for the entire range of concentration employed in this investigation. Figure 8 shows the comparison of equilibrium Cr (VI) uptake by both experimental and Weber-van Vliet Isotherm Model

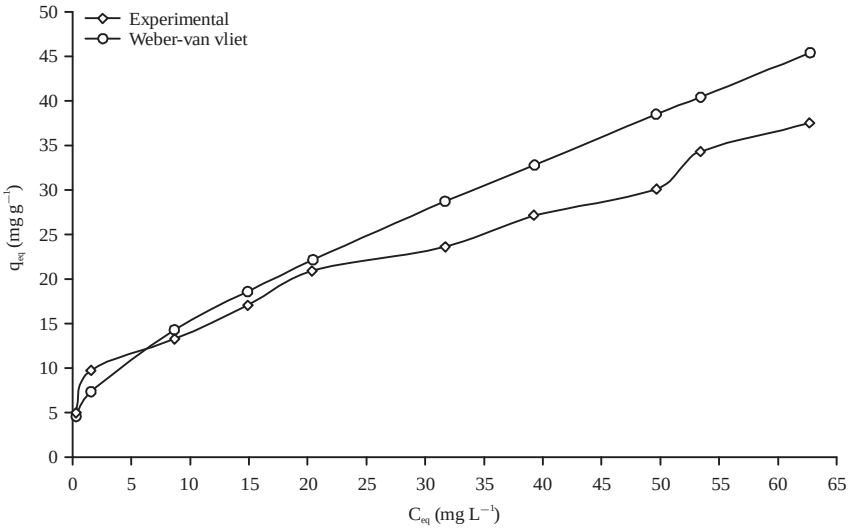

Fig. 8: Comparison of experimental values of equilibrium uptake of Cr (VI) with four parameter model values

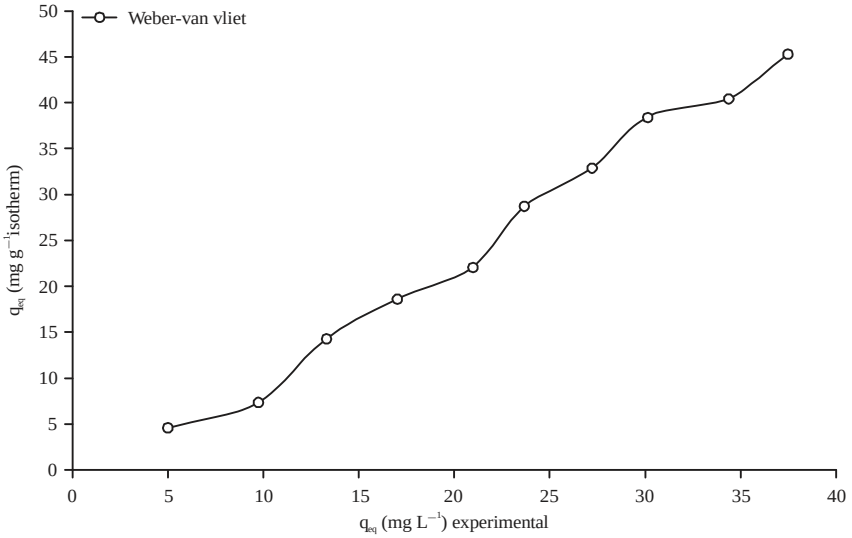

Fig. 9: Accuracy of four parameter model values of equilibrium uptake of Cr (VI) with experimental values

against equilibrium effluent concentration. Upto 120 mg L^{-1} of initial metal ion concentration, the concurrence of model data with experimental data is observed as significant. Thereafter the deviation of model data from the experimental value is high. It is ensured Fig. 9 which shows the experimental and model equilibrium metal uptake upon the initial metal ion concentration. Figure 10 shows the concurrence of equilibrium experimental metal uptake against the Fritz-Schlunder-V adsorption isotherm model data. The values of parameters and regression coefficient R^2 of four parameter adsorption isotherm models for adsorption of Cr (VI) onto BGMA are given in Table 3.

Five parameter model: Table 4 provides the parameter values of Fritz-Schlunder-V parameter model. The R^2 value indicates the significance of this model. Figure 11 shows the comparison of equilibrium Cr (VI) uptake by both experimental and Fritz-Schlunder-V model against equilibrium effluent concentration. For the entire range of concentrations investigated in this study, a significant concurrence of model data with experimental data is observed (Fig. 12). Figure 13 infers more precisely the concurrence of equilibrium experimental metal uptake against the Fritz-Schlunder-V adsorption isotherm model data.

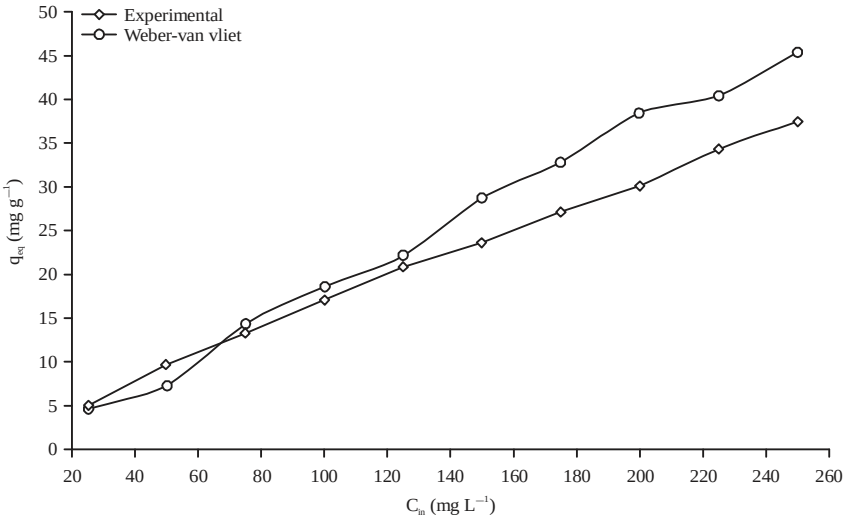

Fig. 10: Concurrence of experimental values of equilibrium uptake of Cr (VI) with four parameter model values upon initial metal ion concentration

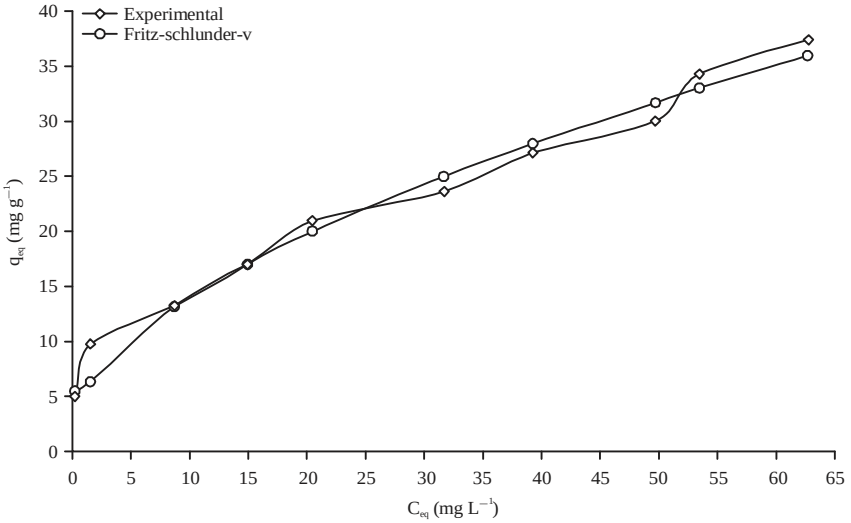

Fig. 11: Comparison of experimental values of equilibrium uptake of Cr (VI) with five parameter model values

Table 3: Parameter values of four parameter adsorption isotherm models for adsorption of Cr (VI) onto BGMA

Models	Parameter	Value	SSE	R^2	Adj R^2	RMSE
Fritz-schlunder-IV isotherm model	A_{FS5}	2599	141.3	0.8627	0.7941	4.852
	B_{FS5}	1809				
	a_{FS5}	-0.5409				
	β_{FS5}	-1.367				
Baudu isotherm model	x	-2.987	119.4	0.884	0.826	4.461
	y	0.8044				
	b_o	1.501×10^4				
	q_{max}	1.627				
Weber-van vliet isotherm model	P1	6.54	12.98	0.9874	0.9811	1.471
	P2	0.2078				
	P3	0.168				
	P4	0.07878				
Marczewski-jaroniec isotherm model	K_{MJ}	1.259×10^4	352.8	0.6572	0.4858	7.668
	m_{MJ}	254				
	n_{MJ}	0.6157				
	q_{max}	28.04				

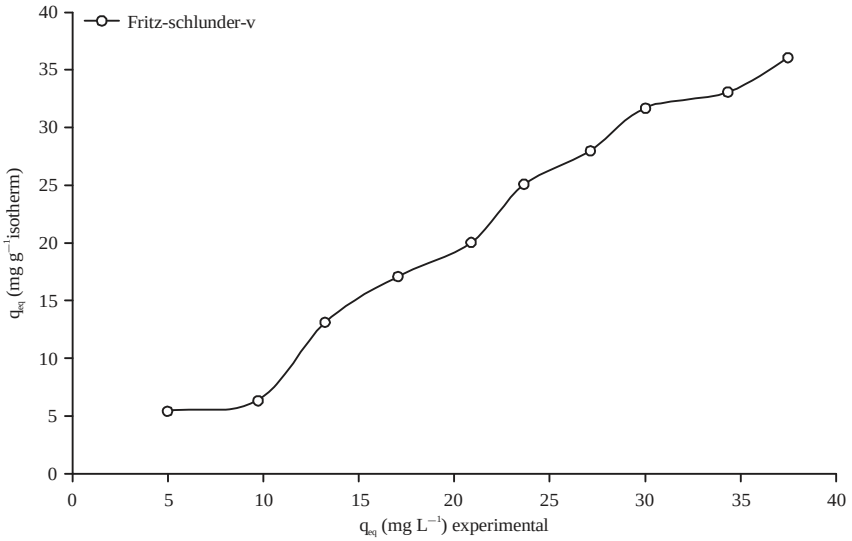

Fig. 12: Concurrence of experimental values of equilibrium uptake of Cr (VI) with five parameter model values upon initial metal ion concentration

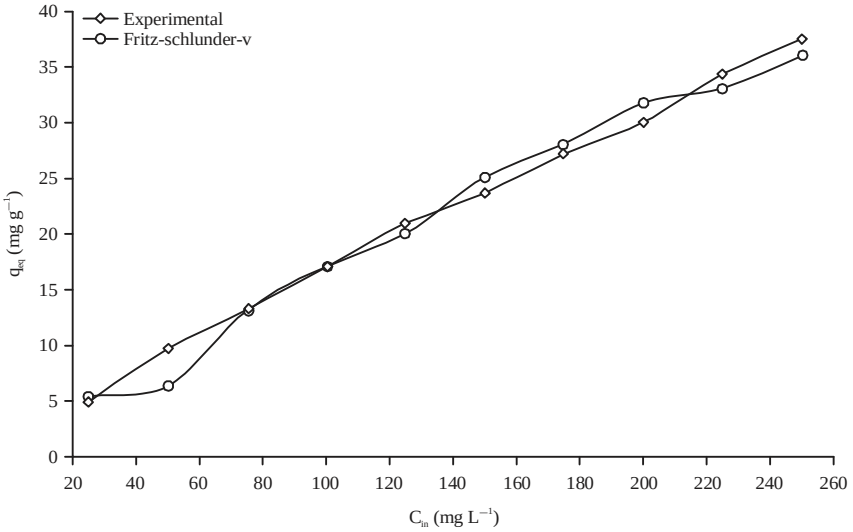

Fig. 13: Accuracy of five parameter model values of equilibrium uptake of Cr (VI) with experimental values

Table 4: Parameter values of five parameter adsorption isotherm model for adsorption of Cr (VI) onto BGMA

Models	Parameter	Value	SSE	R^2	Adj R^2	RMSE
Fritz-schlunder -5 isotherm model	K_{1FS5}	1.355	21.84	0.9788	0.9618	2.09
	K_{2FS5}	-0.7524				
	a_{FS5}	0.6394				
	β_{FS5}	-0.1222				
	q_{max}	1.029				

CONCLUSION

The adsorption of Cr (VI) onto BGMA is found to be L shape. It indicates that no strong competition exists between solvent and the active sites of BGMA to occupy. Freundlich adsorption model is more suitable for the entire range of concentrations investigated in this study. Applicability of Vieth-Sladek isotherm model infers that the adsorption of Cr (VI) onto BGMA is influenced by van der waals forces and ionic forces for the entire range of concentration employed in this investigation.

RECOMMENDATIONS, APPLICATIONS, LIMITATIONS AND FUTURE IMPLICATIONS OF THIS RESEARCH WORK

Blue green algae are recommended to recover the chromium from industrial effluent under the conditions employed in this investigation. The application of the blue green algae is favorable for the recovery of heavy metal ions. The only limitation is the procedure involved in recovery of the adsorbed metal ions by desorption method on industrial scale. In the future study, chemical modification of the algal biomass can be done to enhance the recovery of heavy metal. This can help to reduce the quantity of algae required.

SIGNIFICANCE STATEMENTS

This study discovers the modeling of adsorption isotherms for removal of hexavalent chromium from aqueous solutions using blue green algae with the application of various isotherm models that can be beneficial for gaining insight knowledge of sorbate/sorbent adsorption mechanism which is essential in design of real time operations in industrial scale. Isotherm modeling in adsorption studies is important in identifying or predicting the mechanism of adsorption processes. Hence in this present investigation, various two, three, four and five parameter adsorption isotherm models have been tested.

This study will help the researchers to uncover the critical areas modeling in adsorption that many researchers were not able to explore. Thus this article comprises of critical review of the models with experimental data which would help the readers in acquiring complete knowledge on adsorption mechanisms.

REFERENCES

1. Dehghani, M.H., D. Sanaei, I. Ali and A. Bhatnagar, 2016. Removal of chromium(VI) from aqueous solution using treated waste newspaper as a low-cost adsorbent: Kinetic modeling and isotherm studies. J. Mol. Liquids, 215: 671-679.
2. Amoyaw, P.A., M. Williams and X.R. Bu, 2009. The fast removal of low concentration of cadmium(II) from aqueous media by chelating polymers with salicylaldehyde units. J. Hazard. Mater., 170: 22-26.
3. Aydin, Y.A. and N.D. Aksoy, 2009. Adsorption of chromium on chitosan: Optimization, kinetics and thermodynamics. Chem. Eng. J., 151: 188-194.
4. WHO., 2004. Guidelines for Drinking Water Quality: Recommendations. 3rd Edn., World Health Organization, Geneva, ISBN: 9789241546386, pp: 334.
5. Hena, S., 2010. Removal of chromium hexavalent ion from aqueous solutions using biopolymer chitosan coated with poly 3-methyl thiophene polymer. J. Hazard. Mater., 181: 474-479.
6. Zimmermann, A.C., A. Mecabo, T. Fagundes and C.A. Rodrigues, 2010. Adsorption of Cr(VI) using Fe-crosslinked chitosan complex (Ch-Fe). J. Hazard. Mater., 179: 192-196.
7. Fu, F. and Q. Wang, 2011. Removal of heavy metal ions from wastewaters: A review. J. Environ. Manage., 92: 407-418.
8. Ho, Y.S. and G. McKay, 1998. Sorption of dye from aqueous solution by peat. Chem. Eng. J., 70: 115-124.
9. Hu, X.J., J.S. Wang, Y.G. Liu, X. Li and G.M. Zeng *et al*., 2011. Adsorption of chromium (VI) by ethylenediamine-modified cross-linked magnetic chitosan resin: Isotherms, kinetics and thermodynamics. J. Hazard. Mater., 185: 306-314.
10. Hamadi, N.K., X.D. Chen, M.M. Farid and M.G.Q. Lu, 2001. Adsorption kinetics for the removal of chromium(VI) from aqueous solution by adsorbents derived from used tyres and sawdust. J. Chem. Eng., 84: 95-105.
11. Ouejhani, A., F. Hellal, M. Dachraoui, G. Lalleve and J.F. Fauvarque, 2008. Application of Doehlert matrix to the study of electrochemical oxidation of Cr(III) to Cr(VI) in order to recover chromium from wastewater tanning baths. J. Hazard. Mater., 157: 423-431.
12. Sag, Y and Y. Aktay, 2002. Kinetic studies on sorption of Cr(VI) and Cu(II) ions by chitin, chitosan and *Rhizopus arrhizus*. Biochem. Eng. J., 12: 143-153.
13. Rojas, G., J. Silva, J.A. Flores, A. Rodriguez, M. Ly and H. Maldonado, 2005. Adsorption of chromium onto cross-linked chitosan. Separat. Purificat. Technol., 44: 31-36.
14. Shen, Y.S., S.L. Wang, S.T. Huang, Y.M. Tzou and J.H. Huang, 2010. Biosorption of Cr(VI) by coconut coir: Spectroscopic investigation on the reaction mechanism of Cr(VI) with lignocellulosic material. J. Hazard. Mater., 179: 160-165.
15. Russo, P., A. Catassi, A. Cesario, A. Imperatori and N. Rotolo *et al*., 2005. Molecular mechanisms of hexavalent chromium-induced apoptosis in human bronchoalveolar cells. Am. J. Respir. Cell Mol. Biol., 33: 589-600.
16. Karthikeyan, T., S. Rajgopal and L.R. Miranda, 2005. Chromium(VI) adsorption from aqueous solution by *Hevea brasilinesis* sawdust activated carbon. J. Hazard. Mater., 124: 192-199.
17. Hossain, M.A., M. Kumita, Y. Michigami and S. Mori, 2005. Optimization of parameters for Cr(VI) adsorption on used black tea leaves. Adsorption, 11: 561-568.
18. Gode, F and E. Pehlivan, 2005. Removal of Cr(VI) from aqueous solution by two Lewatit-anion exchange resins. J. Hazard. Mater., 119: 175-182.
19. Park, D., Y.S. Yun and J.M. Park, 2006. Mechanisms of the removal of hexavalent chromium by biomaterials or biomaterial-based activated carbons. J. Hazard. Mater., 137: 1254-1257.

20. Sarin, V. and K.K. Pant, 2006. Removal of chromium from industrial waste by using eucalyptus bark. Bioresour. Technol., 97: 15-20.
21. Baral, S.S., S.N. Dasa and P. Rath, 2006. Hexavalent chromium removal from aqueous solution by adsorption on treated sawdust. Biochem. Eng. J., 31: 216-222.
22. Mohan, D. and C.U. Pittman, Jr., 2006. Activated carbons and low cost adsorbents for remediation of tri-and hexavalent chromium from water. J. Hazard. Mater., 137: 762-811.
23. Sharma, Y.C. and C.H. Weng, 2007. Removal of chromium(VI) from water and wastewater by using riverbed sand: Kinetic and equilibrium studies. J. Hazard. Mater., 142: 449-454.
24. Xing, Y., X. Chen and D. Wang, 2007. Electrically regenerated ion exchange for removal and recovery of Cr(VI) from wastewater. Environ. Sci. Technol., 41: 1439-1443.
25. Foo, K.Y. and B.H. Hameed, 2010. Insights into the modeling of adsorption isotherm systems. Chem. Eng. J., 156: 2-10.
26. Dubey, S.P. and K. Gopal, 2007. Adsorption of chromium(VI) on low cost adsorbents derived from agricultural waste material: A comparative study. J. Hazard. Mater., 145: 465-470.
27. Gode, F. and E. Moral, 2008. Column study on the adsorption of Cr(III) and Cr(VI) using Pumice, Yarikkaya brown coal, Chelex-100 and Lewatit MP 62. Bioresour. Technol., 99: 1981-1991.
28. Baroni, P., R.S. Veira, E. Meneghetti, M.G.C. da Silva and M.M. Beppu, 2008. Evaluation of batch adsorption of chromium ions on natural and crosslinked chitosan membranes. J. Hazard. Mater., 152: 1155-1163.
29. An, H.K., B.Y. Park and D.S. Kim, 2001. Crab shell for the removal of heavy metals from aqueous solution. Water Res., 35: 3551-3556.
30. Selvaraj, K., S. Manonmani and S. Pattabi, 2003. Removal of hexavalent chromium using distillery sludge. Bioresour. Technol., 89: 207-211.
31. Yao, H., L. Guo, B.H. Jiang, J. Luo and X. Shi, 2008. Oxidative stress and chromium(VI) carcinogenesis. J. Environ. Pathol. Toxicol. Oncol., 27: 77-88.
32. Kyzas, G.Z., M. Kostoglou and N.K. Lazaridis, 2009. Copper and chromium(VI) removal by chitosan derivatives-Equilibrium and kinetic studies. Chem. Eng. J., 152: 440-448.
33. Williamas, C.J., D. Aderhold and R.G.J. Edyvean, 1998. Comparison between biosorbents for the removal of metal ions from aqueous solutions. Water, Res., 32: 216-224.
34. Figueira, M.M., B. Volesky, V.S.T. Ciminelli and F.A. Roddick, 2000. Biosorption of metals in brown seaweed biomass. Water Res., 34: 196-204.
35. Aksu, Z., U. Acikel and T. Kutsal, 1999. Investigation of simultaneous biosorption of copper(II) and chromium(VI) on dried *Chlorella vulgaris* from binary metal mixtures: Application of multicomponent adsorption isotherms. Sep. Sci. Technol., 34: 501-524.
36. Aksu, Z. and S. Tezer, 2000. Equilibrium and kinetic modelling of biosorption of Remazol Black B by *Rhizopus arrhizus* in a batch system: Effect of temperature. Process Biochem., 36: 431-439.
37. Aksu, Z., 2005. Application of biosorption for the removal of organic pollutants: A review. Process Biochem., 40: 997-1026.
38. Davis, T.A., B. Volesky and A. Mucci, 2003. A review of the biochemistry of heavy metal biosorption by brown algae. Water Res., 37: 4311-4330.
39. Volesky, B., 1994. Advances in biosorption of metals: Selection of biomass types. FEMS Microbiol. Rev., 14: 291-302.
40. Ayawei, N., A.N. Ebelegi and D. Wankasi, 2017. Modelling and interpretation of adsorption isotherms. J. Chem., Vol. 2017. 10.1155/2017/3039817.
41. Hamdaoui, O. and E. Naffrechoux, 2007. Modeling of adsorption isotherms of phenol and chlorophenols onto granular activated carbon. Part I. Two-parameter models and equations allowing determination of thermodynamic parameters. J. Hazard. Mater., 147: 381-394.
42. Hamdaoui, O. and E. Naffrechoux, 2007. Modeling of adsorption isotherms of phenol and chlorophenols onto granular activated carbon: Part II. Models with more than two parameters. J. Hazard. Mater., 147: 401-411.
43. Al-Sou'od, K., 2012. Adsorption isotherm studies of chromium (VI) from aqueous solutions using Jordanian pottery materials. APCBEE Proc., 1: 116-125.
44. Allen, S.J., G. Mckay and J.F. Porter, 2004. Adsorption isotherm models for basic dye adsorption by peat in single and binary component systems. J. Colloid Interface Sci., 280: 322-333.
45. Samarghandi, M.R., M. Hadi, S. Moayedi and F.B. Askari, 2009. Two-parameter isotherms of methyl orange sorption by pinecone derived activated carbon. Iran. J. Environ. Health Sci. Eng., 6: 285-294.
46. Limousin, G., J.P. Gaudet, L. Charlet, S. Szenknect, V. Barthes and M. Krimissa, 2007. Sorption isotherms: A review on physical bases, modeling and measurement. Applied Geochem., 22: 249-275.
47. Al-Asheh, S., F. Banat, R. Al-Omari and Z. Duvnjak, 2000. Predictions of binary sorption isotherms for the sorption of heavy metals by pine bark using single isotherm data. Chemosphere, 41: 659-665.
48. Mahan, C.A. and J.A. Holcombe, 1992. Immobilization of algae cells on silica gel and their characterization for trace metal preconcentration. Anal. Chem., 64: 1933-1939.
49. Faust, S.D. and M.O. Aly, 1981. Adsorption Processes for Water Treatment. Betterworth Publications, Stoneharm, Massachusetts, USA.
50. Ruthven, D.M., 1984. Principles of Adsorption and Adsorption Processes. John Wiley and Sons, New York, ISBN: 9780471866060, Pages: 433.
51. Langmuir, I., 1916. The constitution and fundamental properties of solids and liquids. Part I. solids. J. Am. Chem. Soc., 38: 2221-2295.

52. Langmuir, I., 1918. The adsorption of gases on plane surfaces of glass, mica and platinum. J. Am. Chem. Soc., 40: 1361-1403.
53. Freundlich, H.M.F., 1906. Uber die adsorption in losungen. Zeitschrift fur Physikalische Chemie, 57: 385-470.
54. Treybal, R.E., 1981. Diffusion and Mass Transfer in Mass-Transfer Operations. 3rd Edn., McGraw-Hill, New York.
55. Dubinin, M.M., 1947. The equation of the characteristic curve of activated charcoal. Dokl. Akad. Nauk. SSSR., 55: 327-329.
56. Radushkevich, L.V., 1949. Potential theory of sorption and structure of carbons. Zhurnal Fizicheskoi Khimii, 23: 1410-1420.
57. Dubinin, M.M., 1960. The potential theory of adsorption of gases and vapors for adsorbents with energetically nonuniform surfaces. Chem. Rev., 60: 235-241.
58. Dubinin, M.M., 1965. Modern state of the theory of volume filling of micropore adsorbents during adsorption of gases and steams on carbon adsorbents. Zhurnal Fizicheskoi Khimii, 39: 1305-1317.
59. Ozcan, A.S., B. Erdem and A. Ozcan, 2005. Adsorption of Acid Blue 193 from aqueous solutions onto BTMA-bentonite. Colloids Surf. A: Physicochem. Eng. Aspects, 266: 73-81.
60. Temkin, M.I. and V. Pyzhev, 1940. Kinetics of ammonia synthesis on promoted iron catalysts. Acta Physicochim. USSR, 12: 327-356.
61. Temkin, M.I., 1941. Adsorption equilibrium and process kinetics on homogeneous surfaces and with interaction between adsorbed molecules. Zh Fiz Khim., 15: 296-332.
62. Hill, T.L., 1946. Statistical mechanics of multimolecular adsorption II. Localized and mobile adsorption and absorption. J. Chem. Phys., 14: 441-453.
63. Hill, T.L., 1952. Theory of physical adsorption. Adv. Catal., 4: 211-258.
64. De Boer, J.H., 1953. The Dynamical Character of Adsorption. Oxford University Press, Oxford.
65. Kumar, P.S., S. Ramalingam, S.D. Kirupha, A. Murugesan, T. Vidhyadevi and S. Sivanesan, 2011. Adsorption behavior of nickel(II) onto cashew nut shell: Equilibrium, thermodynamics, kinetics, mechanism and process design. Chem. Eng. J., 167: 122-131.
66. Sampranpiboon, P., P. Charnkeitkong and X. Feng, 2014. Equilibrium isotherm models for adsorption of zinc (II) ion from aqueous solution on pulp waste. WSEAS Trans. Environ. Dev., 10: 35-47.
67. Amin, M.T., A.A. Alazba and M. Shafiq, 2015. Adsorptive removal of reactive black 5 from wastewater using bentonite clay: Isotherms, kinetics and thermodynamics. Sustainability, 7: 15302-15318.
68. Ebelegi, N.A., S.S. Angaye, N. Ayawei and D. Wankasi, 2017. Removal of congo red from aqueous solutions using fly ash modified with hydrochloric acid. Br. J. Applied Sci. Technol., 20: 1-7.
69. Fowler, R.H. and E.A. Guggenheim, 1939. Statistical Thermodynamics. Cambridge University Press, London, England.
70. Jovanovic, D.S., 1969. Physical adsorption of gases I: Isotherms for monolayer and multilayer adsorption. Kolloid-Zeitschrift Zeitschrift fur Polymere, 235: 1203-1213.
71. Elovich, S.Y. and O.G. Larinov, 1962. Theory of adsorption from solutions of non electrolytes on solid (I) equation adsorption from solutions and the analysis of its simplest form,(II) verification of the equation of adsorption isotherm from solutions. Izv. Akad. Nauk. SSSR. Otd. Khim. Nauk, 2: 209-216.
72. Kiselev, A.V., 1958. Vapor adsorption in the formation of adsorbate molecule complexes on the surface. Kolloid Zhur, 20: 338-348.
73. Hill, A.V., 1910. The possible effects of the aggregation of the molecules of homoglobin on its dissociation curves. J. Physiol., 40: 4-7.
74. Redlich, O. and D.L. Peterson, 1959. A useful adsorption isotherm. J. Phys. Chem., 63: 1024-1024.
75. Sips, R., 1948. On the structure of a catalyst surface. J. Chem. Phys., 16: 490-495.
76. Valenzuela, D.P. and A.L. Myers, 1989. Adsorption Equilibrium Data Handbook. Prentice Hall, Englewood Cliffs, NJ., Pages: 366.
77. Fritz, W. and E.U. Schluender, 1974. Simultaneous adsorption equilibria of organic solutes in dilute aqueous solutions on activated carbon. Chem. Eng. Sci., 29: 1279-1282.
78. Radke, C.J. and J.M. Prausnitz, 1972. Adsorption of organic solutes from dilute aqueous solution of activated carbon. Ind. Eng. Chem. Fund., 11: 445-451.
79. Toth, J., 1971. State equation of the solid-gas interface layers. Acta Chim. Hung., 69: 311-328.
80. Khan, A.R., R. Ataullah and A. Al-Haddad, 1997. Equilibrium adsorption studies of some aromatic pollutants from dilute aqueous solutions on activated carbon at different temperatures. J. Colloid Interface Sci., 194: 154-165.
81. Koble, R.A. and T.E. Corrigan, 1952. Adsorption isotherms for pure hydrocarbons. Ind. Eng. Chem., 44: 383-387.
82. Jossens, L., J.M. Prausnitz, W. Fritz, E.U. Schlunder and A.L. Myers, 1978. Thermodynamics of multi-solute adsorption from dilute aqueous solutions. Chem. Eng. Sci., 33: 1097-1106.
83. Quinones, I. and G. Guiochon, 1996. Derivation and application of a Jovanovic-Freundlich isotherm model for single-component adsorption on heterogeneous surfaces. J. Colloid Interface Sci., 183: 57-67.
84. Brouers, F., O. Sotolongo, F. Marquez and J.P. Pirard, 2005. Microporous and heterogeneous surface adsorption isotherms arising from Levy distributions. Phys. A: Stat. Mech. Applic., 349: 271-282.
85. Ncibi, M.C., S. Altenor, M. Seffen, F. Brouers and S. Gaspard, 2008. Modelling single compound adsorption onto porous and non-porous sorbents using a deformed Weibull exponential isotherm. Chem. Eng. J., 145: 196-202.

86. Vieth, W.R. and K.J. Sladek, 1965. A model for diffusion in a glassy polymer. J. Colloid Sci., 20: 1014-1033.
87. Chern, J.M. and C.Y. Wu, 2001. Desorption of dye from activated carbon beds: effects of temperature, pH and alcohol. Water Res., 35: 4159-4165.
88. Hadi, M., G. McKay, M.R. Samarghandi, A. Maleki and M.S. Aminabad, 2012. Prediction of optimum adsorption isotherm: Comparison of Chi-square and Log-likelihood statistics. Desalination Water Treat., 49: 81-94.
89. Parker, Jr.G.R., 1995. Optimum isotherm equation and thermodynamic interpretation for aqueous 1,1,2-trichloroethene adsorption isotherms on three adsorbents. Adsorption, 1: 113-132.
90. Shahbeig, H., N. Bagheri, S.A. Ghorbanian, A. Hallajisani and S. Poorkarimi, 2013. A new adsorption isotherm model of aqueous solutions on granular activated carbon. World J. Modell. Simulation, 9: 243-254.
91. Baudu, M., 1990. Etude des interactions solutes-fibres de charbon actif: Applications et regeneration. Ph.D. Thesis, University in Rennes, France.
92. Mckay, G., A. Mesdaghinia, S. Nasseri, M. Hadi and M.S. Aminabad, 2014. Optimum isotherms of dyes sorption by activated carbon: Fractional theoretical capacity & error analysis. Chem. Eng. J., 251: 236-247.
93. Van Vliet, B.M., W.J. Weber Jr. and H. Hozumi, 1980. Modeling and prediction of specific compound adsorption by activated carbon and synthetic adsorbents. Water Res., 14: 1719-1728.
94. Sivarajasekar, N. and R. Baskar, 2014. Adsorption of basic red 9 onto activated carbon derived from immature cotton seeds: Isotherm studies and error analysis. Desalin. Water Treat., 52: 7743-7765.
95. Doke, K.M. and E.M. Khan, 2017. Equilibrium, kinetic and diffusion mechanism of Cr(VI) adsorption onto activated carbon derived from wood apple shell. Arabian J. Chem., 10: S252-S260.
96. Gorzin, F. and M.M.B.R. Abadi, 2018. Adsorption of Cr(VI) from aqueous solution by adsorbent prepared from paper mill sludge: Kinetics and thermodynamics studies. Adsorption Sci. Technol., 36: 149-169.
97. Gaffer, A., A.A. Al Kahlawy and D. Aman, 2017. Magnetic zeolite-natural polymer composite for adsorption of chromium (VI). Egypt. J. Petrol., 26: 995-999.
98. Ali, A., K. Saeed and F. Mabood, 2016. Removal of chromium (VI) from aqueous medium using chemically modified banana peels as efficient low-cost adsorbent. Alexandria Eng. J., 55: 2933-2942.
99. Mutongo, F., O. Kuipa and P.K. Kuipa, 2014. Removal of Cr(VI) from aqueous solutions using powder of potato peelings as a low cost sorbent. Bioinorganic Chem. Applic., Vol. 2014. 10.1155/2014/973153.
100. Mulani, K., S. Daniels, K. Rajdeo, S. Tambe and N. Chavan, 2013. Adsorption of chromium (VI) from aqueous solutions by coffee polyphenol-formaldehyde/acetaldehyde resins. J. Polymers, Vol. 2013. 10.1155/2013/798368.
101. Khan, T.A., M. Nazir, I. Ali and A. Kumar, 2017. Removal of chromium(VI) from aqueous solution using guar gum-nano zinc oxide biocomposite adsorbent. Arabian J. Chem., 10: S2388-S2398.
102. Schay, G., 1982. On the definition of interfacial excesses in a system consisting of an insoluble solid adsorbent and a binary liquid mixture. Colloid Polym. Sci., 260: 888-891.
103. Giles, C.H., T.H. MacEwan, S.N. Nakhwa and D. Smith, 1960. Studies in adsorption. Part XI. A system of classification of solution adsorption isotherms and its use in diagnosis of adsorption mechanisms and in measurement of specific surface areas of solids. J. Chem. Soc., 111: 3973-3993.